Nitrogen-doped graphene-ionic liquid-glassy carbon microsphere paste electrode for ultra-sensitive determination of quercetin

Ying Ji[1], Yuan Li[1], Binbin Ren[1], Xinsheng Liu[2,*] Yonghong Li[1,*], Jeffrey Soar[3]

[1]*Electrochemistry and Spectroscopy Analysis Laboratory, School of Public Health and Management, Ningxia Medical University, Yinchuan 750004, P.R. China*

[2]*School of Basic Medical Sciences, Ningxia Medical University, Yinchuan 750004, P.R. China*

[3]*School of Management & Enterprise, University of Southern Queensland, Queensland 4350, Australia*

Abstract: The analysis of quercetin (Qu) is of great significance owing to its multiple biomedical effects. In this work, a nitrogen-doped graphene-ionic liquid-glassy carbon microsphere paste electrode (N-GE/GCILE) was constructed for the determination of Qu. Cyclic voltammetry (CV) and square wave voltammetry (SWV) were employed to investigate the electrochemical behavior of Qu. In comparison with unmodified glassy carbon microsphere paste electrode, the modified electrode exhibited better electrocatalytic activity towards Qu. The influencing conditions on sensitivity such as the amount of modifier, accumulation potential and time, and electrolyte pH value were respectively discussed. Under the optimized conditions, two linear ranges of 0.002- 0.1 μM and 0.1-10 μM were obtained, with a detection limit of 1 nM (S/N=3). The method was applied in Qu determination in blueberry juice with the recoveries of 102.5-105.0 %.

Keywords: Nitrogen-doped graphene; Ionic liquid; Glassy carbon microsphere; Modified electrode; Quercetin.

* Corresponding Author, Tel: +86-951-6980139; Fax: +86-951-6980139.
E-mail: yonghongli2012@163.com (Y. Li); lxs21230@163.com (X. Liu).

1. Introduction

Flavonoids are naturally distributed in fresh fruits, vegetables and other herbs, and usually used as food additives or the ingredient of health products [1, 2]. They exhibit antioxidant, anti-inflammatory and antineoplastic biomedical effects related to radical scavenging properties of such compounds [3, 4]. Quercetin (Qu, the basic chemical structure is shown in Scheme 1) is one of the most important flavonoids, it can be found in onions, celery, sweet pepper, apples, grapes, honeysuckle, pueraria, and other products. The antioxidant capacity of Qu has been extensively demonstrated in the literature [5-7] and it shows other biological benefits including its role as anti-allergic, anti-viral, anti-tumor activity, lowering blood pressure and blood lipids [8, 9]. Therefore, it is important to develop a simple and convenient method for sensitive analysis of Qu.

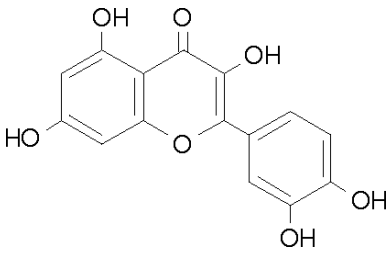

Scheme 1. Chemical structure of quercetin (Qu)

The traditional techniques for detecting Qu involve high-performance liquid chromatography [10, 11], mass spectrometry [12], capillary electrophoresis spectrophotometry [13, 14], and spectrofluorimetry [15]. These traditional methods have high selectivity and sensitivity but are expensive, time-consuming, and they usually need complicated sample pretreatment [16, 17]. Due to the electrochemical activity of Qu, electrochemical methods show potential application in the analysis of Qu and can overcome the shortcomings of the above-mentioned conventional approaches.

The electrochemical technique exhibits the advantages of rapid response, operational simplicity, high sensitivity, and low cost [18]. Some electrochemical sensors were prepared for the detection of Qu; for example, hexadecyltrimethylammonium bromide functionalized Fe decorated MWCNTs

modified carbon paste electrode [19], g-C_3N_4/NiO heterostructured nanocomposite modified glassy carbon electrode [20], and Lewatit FO36 nanoresin/multi-walled carbon nanotubes modified graphite paste electrodes [21] have been used for the electrochemical analysis of Qu.

In order to improve the performance of the modified electrodes, various materials are synthesized. In recent years, chemical doping has gained attention in the field of electrochemistry, it can customize the properties of materials depending on your need. Nitrogen (N) can easily modify the local elemental composition of graphene (GR), and N-functional groups can effectively improve the affinity and binding ability of composite material. This chemically heteroatom-doping in graphene optimizes its surface structure, and enhances the properties of GR electrochemical performance [22-25]. Therefore, nitrogen-doped graphene (N-GE) composite has been extensively applied in the construction of electrochemical sensors ascribed to its excellent characteristics including high electrical conductivity, good chemical stability, superior selectivity for biomolecules and other benefits [26, 27].

Additionally, ionic liquids (ILs) show high conductivity, low volatility, wide electrochemical windows and extensive applicability [28, 29], they can provide an active interface for the electrochemical processes and further modification [30, 31]. Glassy carbon microsphere is also an excellent electrode material with good electrical conductivity, great biocompatibility, high hardness and corrosion resistance [32, 33].

In this paper, a nitrogen-doped graphene-ionic liquid-glassy carbon microsphere paste electrode was firstly prepared (N-GE/GCILE) for Qu analysis. The N-GE with typically crumpled and folded morphologies exhibited large specific surface area, and its special structure could provide plentiful active sites for Qu [34, 35]. With the synergistic effect of N-GE and ILs, the modified electrode presented the increased active surface area and fast electron transfer ability, and it exhibited excellent electrocatalytic activity towards Qu with the negative shift of the oxidation potential. The method had high sensitivity and stability. Finally, the presented method was successfully applied to analyze Qu content in fruit juice samples with satisfactory results.

2. Experimental

2.1. Reagents and materials

The quercetin (Qu) was obtained from Shanghai Aladdin Bio-Chem Technology Co., Ltd. (www.aladdin-e.com) with a purity of 95%. Glassy carbon microsphere (particle diameter: 2-12 μM) was purchased from Sigma-Aldrich (https://www.sigma-aldrich.com), ionic liquid 1-octylpyridinium hexafluorophosphate ($OPPF_6$) was obtained from the Lanzhou Institute of Chemical Physics (http://www.ionicliquid.org) and paraffin oil was obtained from Sinopharm Chemical Reagent Co., Ltd. (http://www. sinoreagent.com). The nitrogen-doped graphene (surface area: >500 m^2/g; nitrogen content: 3.0 wt% ~ 5.0 wt%) was purchased from Nanjing XFNANO Materials Tech Co., Ltd. (http://www.xfnano.com). 0.2 M acetate buffer solution (ABS) was used as a supporting electrolyte prepared by mixing appropriate ratio sodium acetate solution and acetic acid solution. Other chemical reagents involved in the experiment were of analytical grade without further purification.

2.2. Apparatus

CHI660E electrochemical workstation (Shanghai Chenhua Instruments Corporation, http://www.chinstr.com) and PARSTAT 4000 electrochemical workstation (Princeton Applied Research, http://www.par-solartron.com.cn) were used to perform electrochemical measurements. Nitrogen-doped graphene-ionic liquid-glassy carbon microsphere paste electrode (N-GE/GCILE, 3 mm in diameter) was used as the working electrode, saturated calomel electrode (SCE) was the reference electrode, and Pt wire was the auxiliary electrode. An FE20 pH meter (METTLER TOLEDO Instrument Shanghai Co., Ltd., https://www.mt.com) was utilized to measure the pH value of the solution. The test solution was stirred with a magnetic stirrer (Model KMO2, IKA, http://www.ika.cn) during the measurement. Ultrapure water was produced from Heal Force EASY50 water purification system (Shanghai Canrex Analytic Instrument Co., Ltd., http://www.canrex.cn) and used throughout the experiment.

2.3. Electrode preparation

The nitrogen-doped graphene-ionic liquid-glassy carbon microsphere paste electrode (N-GE/GCILE) was prepared by mixing 0.045 g glassy carbon microsphere, 0.005 g nitrogen-doped graphene (N-GE), 0.025 g ionic liquid 1-octylpyridinium hexafluorophosphate ($OPPF_6$) and 15 μL paraffin oil in the mortar. The resulting homogeneous paste was tightly stuffed into the Teflon tube (3.0 mm in diameter), and electrical connection was established by a copper wire. Next, the electrode was heated for at least one minute with a hair dryer. A new surface was obtained by carefully polishing it on a piece of weighing paper.

For comparison, nitrogen-doped graphene modified glassy carbon microsphere paste electrode (N-GE/GCPE) was prepared by mixing glassy carbon microsphere, nitrogen-doped graphene and paraffin oil. Furthermore, glassy carbon microsphere-ionic liquid paste electrode (GCILE) was made up of glassy carbon microsphere, ionic liquid and paraffin oil. And glassy carbon microsphere paste electrode (GCPE) was fabricated with glassy carbon microsphere and paraffin oil.

2.4. Analytical procedure

The electrochemical behavior of Qu was studied by square wave voltammetry (SWV) in 0.2 M ABS solution (pH 4.5) under open-circuit condition. The square wave voltammograms (SWVs) were recorded in the range of 0 V- 0.6 V. And the electrode was rinsed by ultrapure water after each measurement.

2.5. Sample preparation

The real sample was a commercial blueberry juice purchased from a local supermarket. To fit into the linear range, the samples were diluted 100 times by 0.2 M pH 4.5 ABS without any pretreatment before measurement.

3. Results and discussion

3.1. Characterization of the modified electrode

The morphologies and microstructures of bare GCPE, N-GE/GCPE, GCILE, and N-GE/GCILE composites are studied via SEM. As shown in Fig. 1a, the large gap was observed between glassy carbon microspheres on the GCPE. However, GCILE (shown in Fig. 1c) displayed a uniform surface where the ionic liquid was sufficiently filled into the interstice between microspheres due to its high viscosity. As can be seen from Fig. 1b (on N-GE/GCPE), the N-GE was crosslinked with glassy carbon microsphere paste, which exhibited an uneven surface. While in Fig. 1d, the N-GE/GCILE also showed a uniform surface owing to the presence of ionic liquid, and the morphology of N-GE was not visible on the surface, which proved that the modifier was successfully embedded in the matrix.

3.2. Electrochemical properties of the modified electrode

Fig. 2 shows cyclic voltammograms (CVs) of GCPE, N-GE/GCPE, GCILE, and N-GE/GCILE recorded in 5 mM $[Fe(CN)_6]^{3-/4-}$ containing 0.1 M KCl in the range of -0.2 to 0.6 V. As can be seen, the N-GE/GCPE (curve b) showed a remarkable decrease in peak potential separation (ΔEp) and an obvious increase in peak current (Ip) compared with bare GCPE (curve a). When the ionic liquid was added in glassy carbon microsphere paste (GCILE, curve c), peak current obviously increased, meanwhile, the ΔEp further reduced, which indicated the inherent electrocatalysis property of ionic liquid. Furthermore, the highest peak current response was presented on the N-GE/GCILE (curve d). The results verified that N-GE and ionic liquid composites could improve the electrochemical performance of the modified electrode.

Electrochemical impedance spectroscopy (EIS) was employed to further estimate the electron transfer ability of the modified electrodes. Using the $K_3[Fe(CN)_6]$ redox system, the charge transfer resistance (Rct) value can be calculated from the size of the high-frequency semicircle diameter in the Nyquist plots. As seen in Fig. 3, the high electron transfer resistance was observed for GCPE with the Rct value of 2.09

kΩ (curve a). When the N-GE was modified on the electrode, the lower resistance value (Rct=478 Ω) was presented at N-GE/GCPE (curve b). As expected, the N-GE/GCILE (curve c) showed almost a straight line in the Nyquist plots, suggesting that its electron transfer ability was significantly enhanced.

3.3. Surface area study

The effective surface areas of bare GCPE, N-GE/GCPE, GCILE, and N-GE/GCILE were discussed in $K_3[Fe(CN)_6]$ redox system using cyclic voltammetry (CV), which was displayed in Fig. S1. For a reversible process, the relation on peak current and square root of scan rate conforms to the Randles-Sevcik formula [36]:

$$Ipa = (2.69 \times 10^5)\, n^{3/2} A C_0\, D_R^{1/2} \upsilon^{1/2} \qquad (1)$$

where Ipa, A, and υ respectively refers to anodic peak current (A), the effective surface area of the prepared electrode (cm^2) and scan rate ($V\ s^{-1}$); C_0 is the concentration of $K_3[Fe(CN)_6]$ which is equal to 5 mM. In $K_3[Fe(CN)_6]$ redox system, electron transfer number n=1, the diffusion coefficient $D_R=7.6\times10^{-6}$ $cm^2\ s^{-1}$. The surface areas were calculated to be 0.04 cm^2, 0.055 cm^2, 0.106 cm^2 and 0.198cm^2 for GCPE, N-GE/GCPE, GCILE and N-GE/GCILE, respectively. The results indicated that N-GE and ionic liquid could increase the effective surface areas of the modified electrode.

3.4. Electrochemical behaviors of Qu

As shown in Fig. 4, the electrochemical behaviors of 10 μM Qu at GCPE, N-GE/GCPE, GCILE, and N-GE/GCILE were investigated by SWV in 0.2 M ABS (pH 4.5). On the bare GCPE (curve a), a weak oxidation peak (about 16.68 μA) was observed. After N-GE was modified on the electrode, oxidation current (25.02 μA) obviously increased on the N-GE/GCPE (curve b). The phenomenon was attributed to the typically crumpled and folded morphologies of N-GE (the TEM image of N-GE is shown in Fig. 5). It has large specific surface area like graphene, and the nitrogen

doping leads to the distortion of structure with more structural defects, which could provide abundant high edge plane active sites for electrochemical oxidation [34, 35]. Therefore, the electrochemical response was enhanced at N-GE/GCPE. In addition, GCILE (curve c) presented higher current response to Qu (54.51 μA). This was due to ionic liquid could be filled in the gaps between the microspheres and improved electron-transfer kinetics at the prepared electrode [37]. The peak current of Qu on N-GE/GCILE was almost twice higher than that on GCILE. The results indicated that N-GE/GCILE had better electrocatalytic activity towards Qu, which were ascribed to the following factors: Firstly, the micrometer-sized glassy carbon microsphere with large specific surface area can provide more channels for transferring electrons; secondly, due to the CH-π interaction between a CH group of 1-octylpyridinium hexafluorophosphate and π-electrons of N-GE, the ionic liquid could be effectively combined together with N-GE [38], and the composites synergistically promoted electron transfer in the modified electrode; furthermore, N-GE with large surface area exhibited strong adsorption capacity and high electrocatalytic ability to Qu.

3.5. Effect of scan rates

The effect of scan rate (υ) on the oxidation peak current (Ipa) of 10 μM Qu was investigated using CV at the N-GE/GCILE. As shown in Fig. 4, a reversible oxidation peak of Qu was presented, and Ipa increased as the increasing scan rate (υ) with a slight positive shift in oxidation peak potential (Epa) in the scan rates range of 25- 400 mV s^{-1}. The insert in Fig. 6 exhibited peak current was proportional to scan rate with a linear regression equation of Ipa (μA) =0.1262 υ (mV s^{-1}) - 0.4629(r^2=0.9999), which confirmed an adsorption-controlled process for the electrochemical oxidation of Qu at the N-GE/GCILE.

3.6. Optimization of analytical conditions

3.6.1. Effect of pH value

The effects of pH value on the oxidation peak current (Ipa) and peak potential (Epa) of 10 μM Qu were discussed. Fig. S2 exhibits SWVs of 10 μM Qu in 0.2 M ABS with the pH range of 2.5-6.0. As shown in the figure, the Epa shifted towards negative position as the pH value of supporting electrolyte increased, and the linear relationship of Epa and pH value was described as follows: Epa (V) = - 0.07 pH+0.61 (r=0.9922). The slope value of 70 mV pH^{-1} deviated from the theoretical value. According to the Nernst equation, it may be attributed to the properties of the constructed electrode and the influence of the temperature. This finding was consistent with the results in previous reports [39, 40], 70 mV pH^{-1} was considered to be close to the theoretical value, suggesting that the number of transferred electrons and protons involved in the electrochemical process of Qu was equal [41]. Furthermore, as the pH value increased from 2.5 to 4.5, the current response of Qu increased. However, the further increase of the pH value led to the gradual decrease of peak current. The results may be stated by the following reasons: at higher pH values, the deprotonation of Qu influences the accumulation of Qu at the electrode surface and electrochemical reaction. On the contrary, the hydroxyl groups of Qu are active at lower pH values [42]. Therefore, 0.2 M pH 4.5 ABS was chosen as supporting electrolyte in the next experiment.

3.6.2. Effect of the amount of the modifier

The effect of the amount of the N-GE on the voltammetric response towards 10 μM Qu was investigated. In Fig. S3, the current response increased with the increasing amount of N-GE from 0 to 2.5%, and reached the maximum as the amount of modifier was 2.5%. Then a gradual decrease on the response signal was observed when the proportion of N-GE exceeded 2.5%. The rising trend in current response could be ascribed to the large electroactive surface area and the improved absorption capacity when a certain amount of N-GE was modified on the electrode. However, excessive N-GE in the paste would increase the film thickness, block the electron

transfer and then influenced the oxidation process of Qu. Therefore, 2.5 wt% N-GE was chosen for preparation of the modified electrode in the subsequent experiments.

3.6.3. Effect of accumulation potential and accumulation time

The influence of the accumulation potential and open-circuit condition on the voltammetric response was discussed under the same experimental conditions (not shown). The response signal showed no significant difference between an accumulation potential and an open-circuit condition, so the open-circuit condition was selected in the follow-up experiment. The obtained results had confirmed that the oxidation of Qu at N-GE/GCILE was a typical adsorption-controlled process, thence accumulation time was a key factor on current response of Qu. As shown in Fig. S4, with the accumulation time varied from 10 to 180 s, the current response increased gradually because more Qu was adsorbed on the electrode surface. After 180 s, the peak current changed a little because the adsorption of Qu reached saturation. Ultimately, the accumulation process of Qu was performed at 180 s under open-circuit condition considering sensitivity and work efficiency of analysis.

3.7. Determination of Qu

The SWV was used to determine Qu at the N-GE/GCILE. Fig. 7 exhibits SWVs of different concentrations of Qu. From Fig. 7A, peak currents gradually increased with the increasing concentrations. Two linear ranges were obtained in Fig. 7B and Fig. 7C, they were 0.002-0.1 μM and 0.1-10 μM, respectively; and the linear regression equations were: Ipa (μA) = 49.5354 c (μM) + 0.1528 (r^2=0.9984) and Ipa (μA) = 6.3114 c (μM) + 4.4662 (r^2=0.9985), respectively. The limit of detection (LOD) was calculated as 1 nM (S/N=3). Furthermore, the better analysis parameters were achieved at N-GE/GCILE in comparison to other reported analytical methods [20, 21, 43-45]. Table 1 summarizes the key parameters of various modified electrodes for Qu detection.

3.8. Reproducibility and stability

The reproducibility and stability of the N-GE/GCILE were investigated in the presence of 10 μM Qu. The relative standard deviation (RSD) was calculated to be 1.35% by six repetitive measurements using the same electrode. Similarly, for six modified electrodes prepared in the same procedure, the RSD was 2.37%. The results exhibited good reproducibility of the modified electrode. Moreover, the current response of Qu retained 98.3% of the initial value after one month under room temperature, confirming the outstanding stability of the sensor.

3.9. Selectivity

Some potential interfering substances were measured on the detection of Qu (not shown). The results showed that common inorganic interferences, such as 500-fold excess of K^+, Na^+, Mg^{2+}, Pb^{2+}, NO_3^-, Cl^-, 400-fold concentration of Co^{2+} and 200-fold concentration of Ca^{2+}, Cu^{2+}, Al^{3+}, Cr^{3+} had no interference on the detection of Qu. Furthermore, the response of Qu was hardly interfered by some organic substances, including 500-fold glucose, 400-fold cystine, tyrosine, 200-fold glycine, arginine, 100-fold ascorbic acid, 50-fold dopamine, uric acid, and the same concentration of luteolin and rutin (the current value changed less than ± 5%). The analysis method could be used for selective determination of Qu with outstanding anti-interference ability.

4. Real sample analysis

The analysis of blueberry juice was undertaken using the proposed method in order to evaluate the practicality of the modified electrode. The standard addition method was used, and the results were summarized in Table 2. The recoveries ranged from 102.5% to 105.0%, and the RSD was found to be less than 1.85%, suggesting that the method had significant potential for practical application.

5. Conclusions

In this work, we have developed a nitrogen-doped graphene-ionic liquid-glassy carbon microsphere paste electrode by a simple fabrication procedure. The modified electrode exhibited excellent electrocatalytic performance towards Qu compared to other electrodes. The method provided wide linear ranges (0.002-0.1 μM and 0.1-10 μM), low detection limit (1 nM), good reproducibility, stability, and high selectivity. The fabricated electrode was successfully applied for Qu detection in blueberry juice with satisfactory recoveries. The results confirmed the feasibility of the modified electrode for the determination of Qu in food samples.

Acknowledgements This research was supported by the Top Discipline of Public Health and Prevent Medicine (No. NXYLXK2017B08), Education Department of Ningxia, China, and China Scholarship Council (No. 201808645034).

References

[1] S.B. Nimse, D. Pal, Free radicals, natural antioxidants, and their reaction mechanisms, RSC Adv 5 (2015) 27986–28006.

[2] C.Q. Liu, J.Z. Huang, L.S. Wang, Electrochemical synthesis of a nanocomposite consisting of carboxy-modified multi-walled carbon nanotubes, polythionine and platinum nanoparticles for simultaneous voltammetric determination of myricetin and rutin, Microchim Acta 185 (2018) 414.

[3] S. Tajyani, A. Babaei, A new sensing platform based on magnetic Fe3O4@NiO core/shell nanoparticles modified carbon paste electrode for simultaneous voltammetric determination of Quercetin and Tryptophan, J Electroanal Chem 808 (2018) 50–58.

[4] S. Sen, R. Chakraborty, The role of antioxidants in human health, ACS Symp Ser 1083 (2011) 1–37.

[5] J. Manokaran, R. Muruganantham, A. Muthukrishnaraj, N. Balasubramanian, Platinum-polydopamine@SiO_2 nanocomposite modified electrode for the electrochemical determination of quercetin, Electrochim Acta 168 (2015) 16–24.

[6] S.K. Ponnaiah, P. Periakaruppan, A glassy carbon electrode modified with a copper tungstate and polyaniline nanocomposite for voltammetric determination of quercetin, Microchim Acta 185 (2018) 524.

[7] L. Tian, B.B. Wang, R.Z. Chen, Y. Gao, Y.L. Chen, T. J. Li, Determination of quercetin using a photo-electrochemical sensor modified with titanium dioxide and a platinum (II)-porphyrin complex, Microchim Acta 182 (2015) 687–693.

[8] S.M. Ghoreishi, S. Masoum, M. Mosleh, A. Khoobi, Determination of quercetin in the presence of tannic acid in soft drinks based on carbon nanotubes modified electrode using chemometric approaches, Sensor Actuat B 272 (2018) 605-611.

[9] Z.F. Yao, X. Yang, X.B. Liu, Y.Q. Yang, Y.J. Hu, Z.J. Zhao, Electrochemical quercetin sensor based on a nanocomposite consisting of magnetized reduced graphene oxide, silver nanoparticles and a molecularly imprinted polymer on a screen-printed electrode, Microchim Acta 185 (2018) 70.

[10] J. Jing, Y.Z. Shi, Q.F. Zhang, J. Wang, J.R. Ruan, Prediction of Chinese green tea ranking by

metabolite profiling using ultra-performance liquid chromatography-quadrupole time-of-flight mass spectrometry (UPLC-Q-TOF/MS), Food Chem 221 (2017) 311-316.

[11] L.M. Berger, S. Wein, R. Blank, C.C. Metges, S. Wolffram, Bioavailability of the flavonol quercetin in cows after intraruminal application of quercetin aglycone and rutin, J Dairy Sci 95 (2012) 5047–5055.

[12] V. Pilařová, K. Plachká, L. Chrenková, I. Najmanová, P. Mladěnka, F. Švec, O. Novák, L. Nováková, Simultaneous determination of quercetin and its metabolites in rat plasma by using ultra-high performance liquid chromatography tandem mass spectrometry, Talanta 185 (2018) 71-79.

[13] R.T. Johnson, C.E. Lunte, A capillary electrophoresis electrospray ionization-mass spectrometry method using a borate background electrolyte for the fingerprinting analysis of flavonoids in Ginkgo biloba herbal supplements, Anal Methods 8 (2016) 3325–3332.

[14] L.R. Tallini, G.P.R. Pedrazza, S.A.L. Bordignon, A.C.O. Costa, M. Steppe, A. Fuentefria, J.A.S. Zuanazzi, Analysis of flavonoids in rubusery throcladus and morus nigraleaves extracts by liquid chromatography and capillary electrophoresis, Rev Bras Farmacognosia 25 (2015) 219–227.

[15] R. Ravichandran, M. Rajendran, D. Devapiriam, Antioxidant study of quercetin and their metal complex and determination of stability constant by spectrophotometry method, Food Chem146 (2014) 472–478.

[16] H.M. Qiu, C.N. Luo, M. Sun, F.G. Lu, L.L. Fan, X.J. Li, A novel chemiluminescence sensor for determination of quercetin based on molecularly imprinted polymeric microspheres, Food Chem 134 (2012) 469–473.

[17] A.A. Abdullah, Y. Yardım, Z. Şentürk, The performance of cathodically pretreated boron-doped diamond electrode in cationic surfactant media for enhancing the adsorptive stripping voltammetric determination of catechol-containing flavonoid quercetin in apple juice, Talanta 187 (2018) 156-164.

[18] X.G. Chen, R. Wang, G.F. Zhao, X.Y. Zou, Electrocatalytic oxidation and determination of ascorbic acid on polymer hydroquinone modified electrode, Chinese J Anal Chem 34 (2006) 1063-1106.

[19] V. Erady, R.J. Mascarenhas, A.K. Satpati, S. Detriche, Z. Mekhalif, J. Delhalle, A. Dhason, A novel and sensitive hexadecyltrimethylammoniumbromide functionalized Fe decorated MWCNTs modified carbon paste electrode for the selective determination of Quercetin, Mat Sci Eng C 76 (2017) 114–122.

[20] S. Selvarajan, A. Suganthi, M. Rajarajan, Fabrication of g-C_3N_4/NiO heterostructured nanocomposite modified glassy carbon electrode for quercetin biosensor, Ultrason Sonochem 41 (2018) 651–660.

[21] H. Rajabi, M. Noroozifar, Modified graphite paste electrode with Lewatit FO36 Nanoresin/multi-walled carbon nanotubes for determination of quercetin, Russ J Electrochem 54 (2018) 234-242.

[22] X.L. Niu, X.Y. Li, H. Xie, Y. Cheng, W. Sun, Y.Q. Huang, Y.L. Men and L.F. Dong, Electrocatalytic detection of uric acid on nitrogen-doped graphene modified electrode and its application, J Chin Chem Soc-Taip 64 (2017) 1360-1366.

[23] Y. Hao, X.F. Li, X.L. Sun, C.L. Wang, Nitrogen-doped graphene nanosheets/Sulfur composites as cathode in room-temperature sodium-sulfur batteries, ChemistrySelect 2 (2017) 9425–9432.

[24] R. Singh, M. Kumar, H. Khajuria, S. Sharma, H.N. Sheikh, Studies on hydrothermal synthesis of photolumniscent rare earth (Eu^{3+} & Tb^{3+}) doped NG@$FeMoO_4$ for enhanced visible light photodegradation of methylene blue dye, Solid State Sci 76 (2018) 38–47.

[25] S. Ai, Y.X. Chen, Y.L. Liu, Q. Zhang, L.J. Xiong, H.B. Huang, L. Li, X.H. Yu, L. Wei, Facile synthesis of nitrogen-doped graphene aerogels for electrochemical detection of dopamine, Solid State Sci 86 (2018) 6–11.

[26] M. Kaur, M. Kaur, V.K. Sharma, Nitrogen-doped graphene and graphene quantum dots: A review on synthesis and applications in energy, sensors and environment, Adv Colloid Interface Sci 259 (2018) 44–64.

[27] Liu R, Wu D, Feng X, Mullen K, Nitrogen-doped ordered mesoporous graphitic arrays with high electrocatalytic activity for oxygen reduction, Angew Chem Int Ed 49 (2010) 2565.

[28] B.J. Xu, L.T. Yang, F.Q. Zhao, B.Z. Zeng, A novel electrochemical quercetin sensor based on Pd/MoS_2-ionic liquid functionalized ordered mesoporous carbon, Electrochim Acta 247 (2017) 657-665.

[29] E. Nagles, O. García-Beltrán, J.A. Calderón, Evaluation of the usefulness of a novel electrochemical sensor in detecting uric acid and dopamine in the presence of ascorbic acid using a screen-printed carbon electrode modified with single walled carbon nanotubes and ionic liquids, Electrochim Acta 258 (2017) 512-523.

[30] Y.H. Li, Y. Ji, B.B. Ren, L.N. Jia, G.D. Ma, X.S. Liu, Carboxyl-functionalized mesoporous molecular sieve/colloidal gold modified nano-carbon ionic liquid paste electrode for electrochemical determination of serotonin, Mater Res Bull 109 (2019) 240–245.

[31] Y.H. Li, X.R. Zhai, X.S. Liu, L. Wang, H.R. Liu, H.B. Wang, Electrochemical determination of bisphenol A at ordered mesoporous carbon modified nano-carbon ionic liquid paste electrode, Talanta 148 (2016) 362–369.

[32] J.C. Ruiz-Morales, J. Canales-Va´zquez, D. Marrero-Lo´pez, S.N. Savvin, P. Nu´nez, A.J. Dos Santos-Garcı´a, C. Sa´nchez-Bautista, J. Pen˜a-Martı´nez, Fabrication of 3D carbon microstructures using glassy carbon microspheres and organic precursors, Carbon 48 (2010) 3964-3967.

[33] H. Ibrahim, Y. Temerk, A novel electrochemical sensor based on B doped CeO_2 nanocubes modified glassy carbon microspheres paste electrode for individual and simultaneous determination of xanthine and hypoxanthine, Sensor Actuat B 232 (2016) 125-137.

[34] X.Q. Li, H.L. Zhao, L.B. Shi, X. Zhu, M.B. Lan, Q. Zhang, Z.H. Fan, Electrochemical sensing of nicotine using screen-printed carbon electrodes modified with nitrogen-doped graphene sheets, J Electroanal Chem784 (2017) 77–84.

[35] S. Mutyala, J. Mathiyarasu, A highly sensitive NADH biosensor using nitrogen doped graphene modified electrodes, J Electroanal Chem 775 (2016) 329–336.

[36] Y.H. Li, X.R. Zhai, H.B. Wang, X.S. Liu, L. Guo, X.L. Ji, L. Wang, H.Y. Qiu, X.Y. Liu, Non-enzymatic sensing of uric acid using a carbon nanotube ionic-liquid paste electrode modified with poly(β-cyclodextrin), Microchim Acta 182 (2015) 1877-1884.

[37] H. Dai, H.F. Xu, X.P. Wu, Y.W. Chi, G.N. Chen, Fabrication of a new electrochemiluminescent sensor for fentanyl citrate based on glassy carbon microspheres and ionic liquid composite paste electrode, Anal Chim Acta 647 (2009) 60–65.

[38] Y.Y. Shea, J.F. Chen, C.X. Zhang, Z.G. Lu, M. Ni, Patrick H.-L. Sit, Michael K.H. Leung, Oxygen Reduction Reaction Mechanism of Nitrogen-Doped Graphene Derived from Ionic

Liquid, Energy Procedia 142 (2017) 1319–1326.

[39] J.T. Qiao, Y.L. Zhang, S. Lei, Z. Liu, G.P. Li, B.X. Ye, Sensitive determination of baicalein based on functionalized graphene loaded RuO_2 nanoparticles modified glassy carbon electrode, Talanta 188 (2018) 714–721.

[40] Z.K. Xie, G.P. Li, Y.M. Fu, M.J. Sun, B.X. Ye, Sensitive, simultaneous determination of chrysin and baicalein based on Ta_2O_5-chitosan composite modified carbon paste electrode, Talanta 165 (2017) 553–562.

[41] X.L. Niu, X.Y. Lia, W. Chen, X.B. Li, W.J. Weng, C.X. Yin, R.X. Dong, W. Sun, G.J. Li, Three-dimensional reduced graphene oxide aerogel modified electrode for the sensitive quercetin sensing and its application, Mat Sci Eng C 89 (2018) 230–236.

[42] P. Xiao, F.Q. Zhao, B.Z. Zeng, Voltammetric determination of quercetin at a multi-walled carbon nanotubes paste electrode, Microchem J 85 (2007) 244–249.

[43] J. Li, J. Qu, R. Yang, L. Qu, P. D. B. Harrington, A sensitive and selective electrochemical sensor based on graphene quantum dot/gold nanoparticle nanocomposite modified electrode for the determination of quercetin in biological samples, Electroanal 28 (2016) 1–10.

[44] A. S¸enocak , B. K¨oksoy, E. Demirbas¸, T. Basova, M. Durmus¸, 3D SWCNTs-coumarin hybrid material for ultra-sensitive determination of quercetin antioxidant capacity, Sensor Actuat B 267 (2018) 165-173.

[45] J. Manokaran, R. Muruganantham, A. Muthukrishnaraj, N. Balasubramanian, Platinum-polydopamine @SiO_2 nanocomposite modified electrode for the electrochemical determination of quercetin, Electrochim Acta 168 (2015) 16–24.

Figure captions

Fig.1. SEM images of (a) GCPE, (b) N-GE/GCPE, (c) GCILE and (d) N-GE/GCILE.

Fig.2. Cyclic voltammograms of 5 mM $[Fe(CN)_6]^{3-/4-}$ containing 0.1 M KCl at GCPE (a), N-GE/GCPE(b), GCILE(c) and N-GE/GCILE(d), respectively, with a scan rate of 50 mV s^{-1}.

Fig.3. Nyquist plots of 5 mM $[Fe(CN)_6]^{3-/4-}$ containing 0.1 M KCl at GCPE (a), N-GE/GCPE(b) and N-GE/GCILE(c).

Fig.4. SWVs of 10 μM quercetin in 0.2 M ABS (pH 4.5) at the (a) GCPE, (b) N-GE/GCPE, (c) GCILE and (d) N-GE/GCILE.

Fig.5. TEM image of N-GE.

Fig.6. Cyclic voltammograms of 10 μM quercetin in 0.2 M ABS (pH 4.5) at the N-GE/GCILE at scan rate of 25, 50, 100, 150, 200, 250, 300, 350, 400 mV s^{-1} (from inner to outer); The insert is the relationship between the peak currents and scan rates.

Fig.7. (A) SWVs for different concentrations of quercetin (from bottom to top: 0, 0.001, 0.002, 0.005, 0.01, 0.05, 0.1, 0.5, 1, 5, 10 μM quercetin; the amplified SWVs for quercetin in lower concentrations are shown in the insert); (B) The relationship between the peak currents and the quercetin concentration in the range of 0.002-0.1 μM; (C) The relationship between the peak currents and the quercetin concentration in the range of 0.1-10 μM (the error bars were derived from the standard deviation of two parallel measurements).

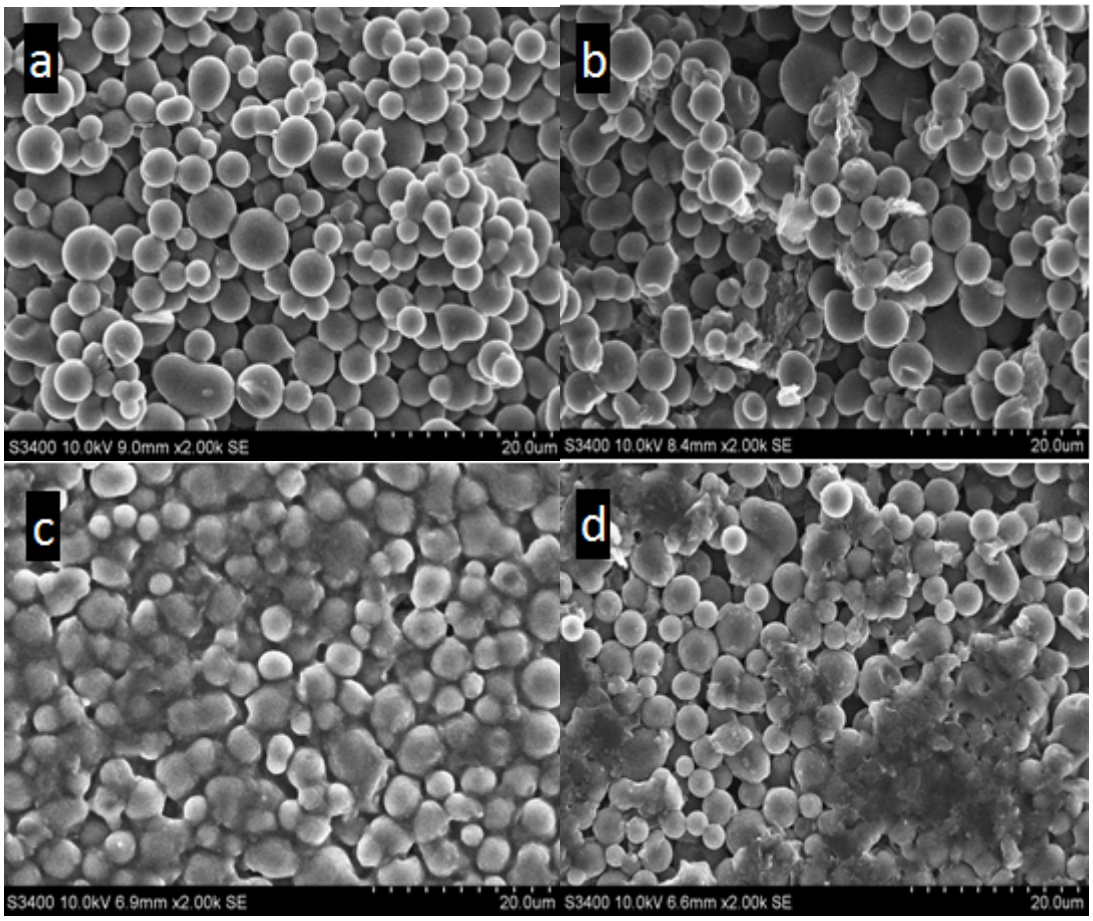
a
b
S3400 10.0kV 9.0mm x2.00k SE
20.0um
S3400 10.0kV 8.4mm x2.00k SE
20.0um
c
d
S3400 10.0kV 6.9mm x2.00k SE
20.0um
S3400 10.0kV 6.6mm x2.00k SE
20.0um

Fig. 1

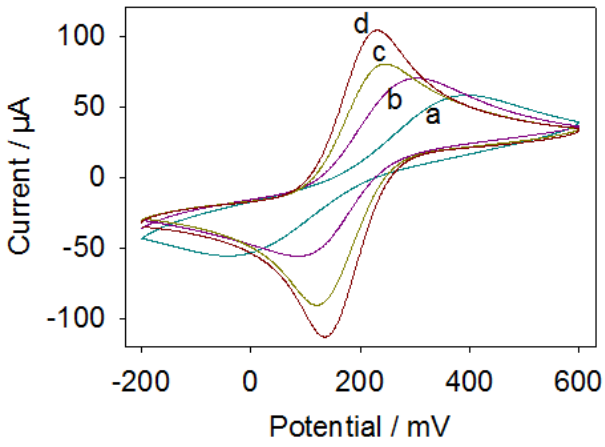

Fig. 2

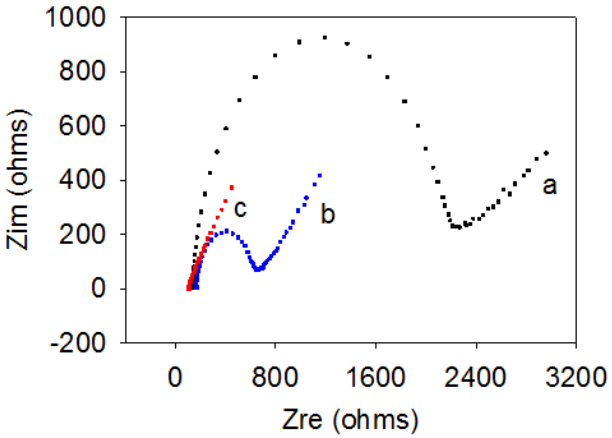
1000
800
600
400
200
0
-200
Zim (ohms)
0
800
1600
2400
3200
Zre (ohms)
a
b
c

Fig. 3

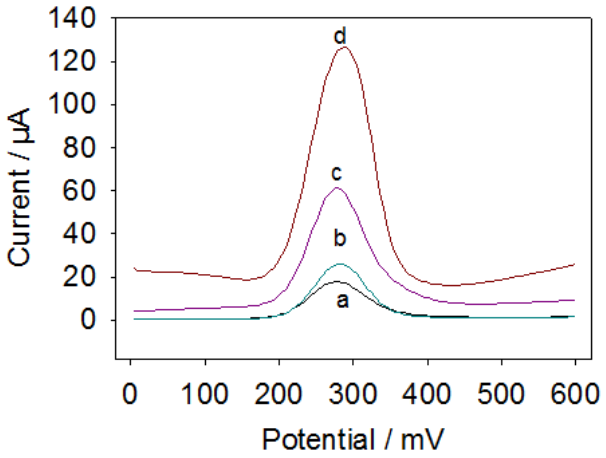
Current / μA
Potential / mV
0
20
40
60
80
100
120
140
0
100
200
300
400
500
600
a
b
c
d

Fig. 4

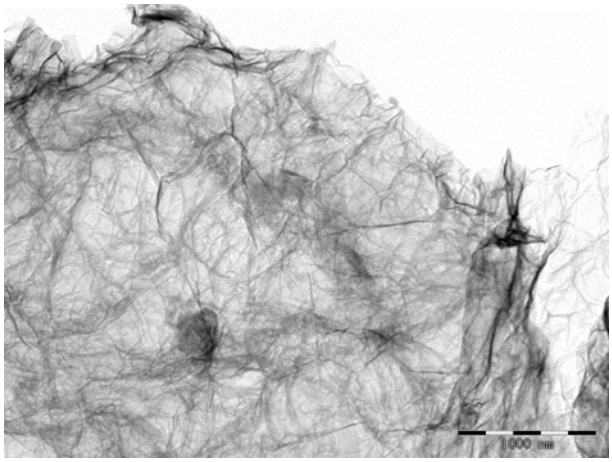

Fig. 5

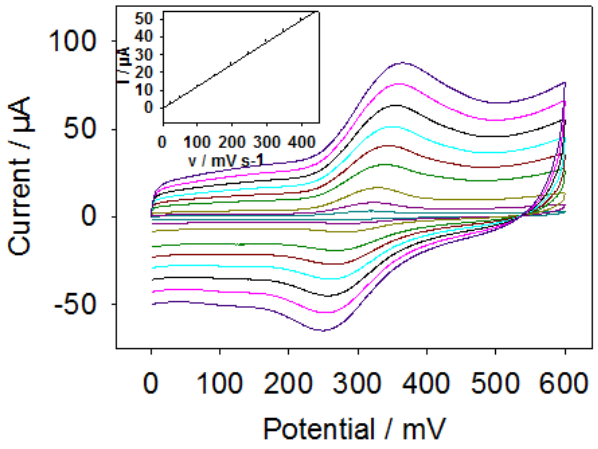
Current / µA
100
50
0
-50
0
100
200
300
400
500
600
Potential / mV
I / µA
50
40
30
20
10
0
0
100
200
300
400
v / mV s-1

Fig. 6

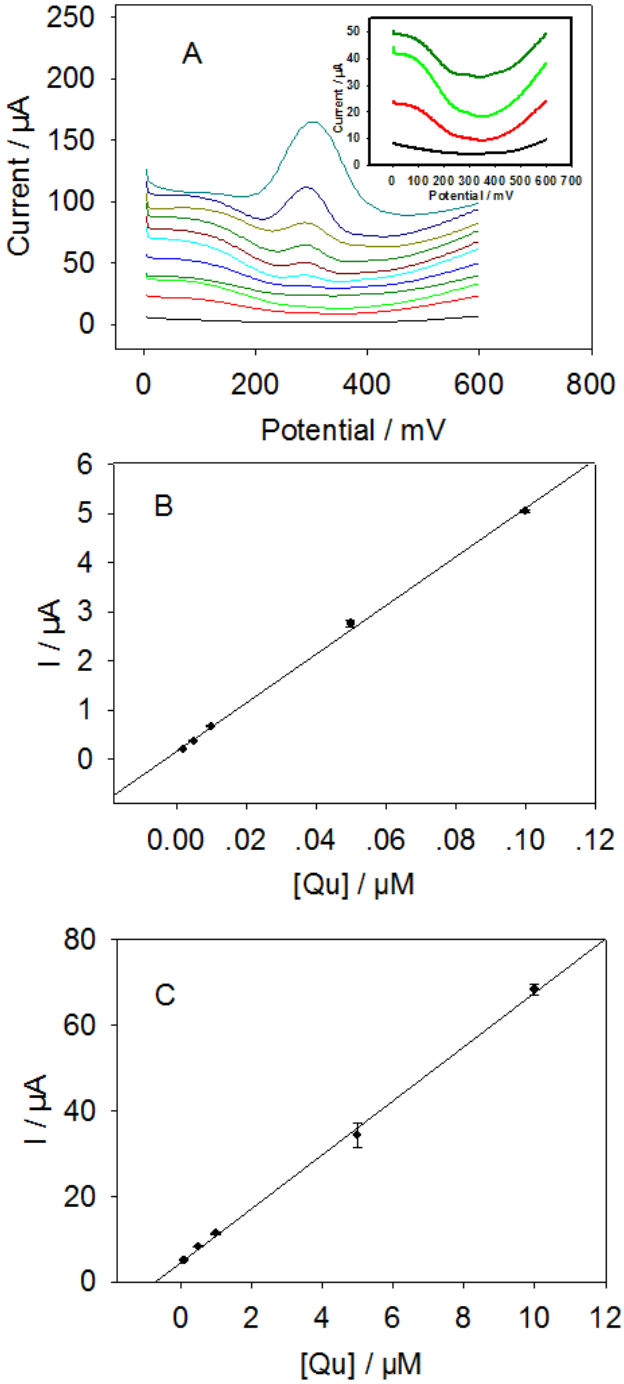
A
Current / μA
Potential / mV
Current / μA
Potential / mV
B
I / μA
[Qu] / μM
C
I / μA
[Qu] / μM

Fig. 7

Table 1 Comparison of analysis parameters of Qu detection for various modified electrodes

Modified electrode	Method	Linear range (μM)	Limit of detection (μM)	Reference
g-C_3N_4/NiO/GCE	DPV	0.010 – 250	0.002	20
LFONR-MWCNT/GPE	LSV	1.8–25/25-570	0.213	21
GOD/AuNP/GCE	DPV	0.01–6	0.002	43
3D-coumarin-SWCNTs/GCE	DPSV	0.25–3	0. 020	44
Pt-PDA@SiO_2/GCE	SWV	0.05 -0.383	0.016	45
N-GE/GCILE	SWV	0.002-0.1/0.1-10	0.001	This work

g-C_3N_4: Graphitic carbon nitride; NiO: nickel oxide; GCE: glassy carbon electrode; DPV: differential pulse voltammetry; LFONR: Lewatit FO36 nanoresin; MWCNT: multi-walled carbon nanotube; GPE: graphite paste electrode; LSV: linear sweep voltammetry; GOD: graphene quantum dot; AuNP: gold nanoparticle; 3D: a three-dimensional architecture; SWCNTs: single walled carbon nanotubes; DPSV: differential pulse stripping voltammetry; Pt-PDA@SiO_2: platinum-polydopamine coated silica particles; SWV: square wave voltammetry; N-GE: nitrogen-doped graphene; GCILE: ionic liquid-glassy carbon microspheres paste electrode

Table 2 Determination of quercetin in blueberry juice samples using N-GE/GCILE (n=3[a])

	Sample 1	Sample 2	Sample 3
Detected /μM	2.68	2.48	2.53
Added /μM	2.00	2.00	2.00
Found /μM	4.74	4.58	4.58
Recovery / %	103.0	105.0	102.5
R.S.D. / %	1.64	1.85	1.59

[a] Three different measurements were made for each sample.

Electronic Supplementary Material

Nitrogen-doped graphene-ionic liquid-glassy carbon microspheres paste electrode for ultra-sensitive determination of quercetin

Ying Ji[1], Yuan Li[1], Binbin Ren[1], Xinsheng Liu[2,*] Yonghong Li[1,*], Jeffrey Soar[3]

[1]*Electrochemistry and Spectroscopy Analysis Laboratory, School of Public Health and Management, Ningxia Medical University, Yinchuan 750004, P.R. China*

[2]*School of Basic Medical Sciences, Ningxia Medical University, Yinchuan 750004, P.R. China*

[3]*School of Management & Enterprise, University of Southern Queensland, Queensland 4350, Australia*

[*] Corresponding Author, Tel: +86-951-6980139; Fax: +86-951-6980139.
E-mail: yonghongli2012@163.com (Y. Li); lxs21230@163.com (X. Liu).

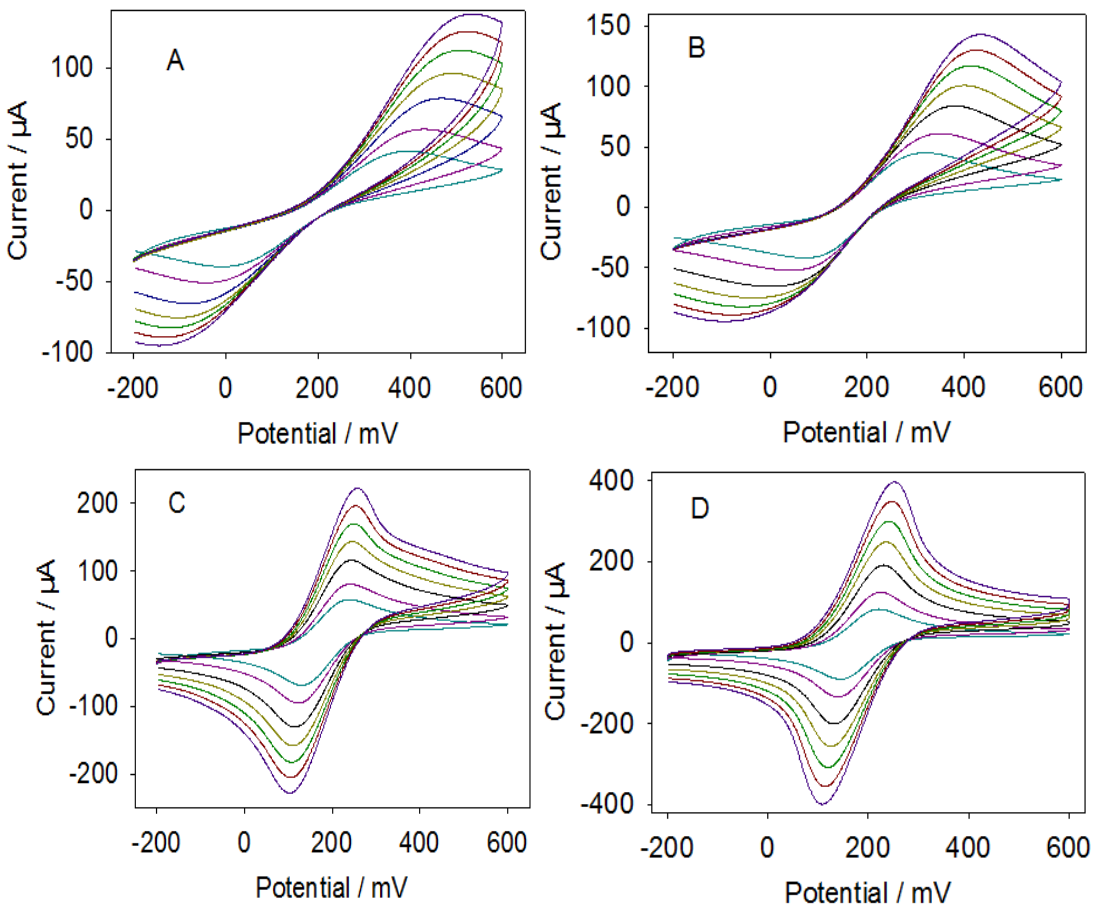

Fig. S1 Cyclic voltammograms of GCPE(A), N-GE/GCPE(B), GCILE(C), N-GE/GCILE(D) in 5mM $[Fe(CN)_6]^{3-/4-}$ containing 0.1M KCl at scan rate of 25,50,100,150,200, 250, 300mVs^{-1}(from inner to outer).

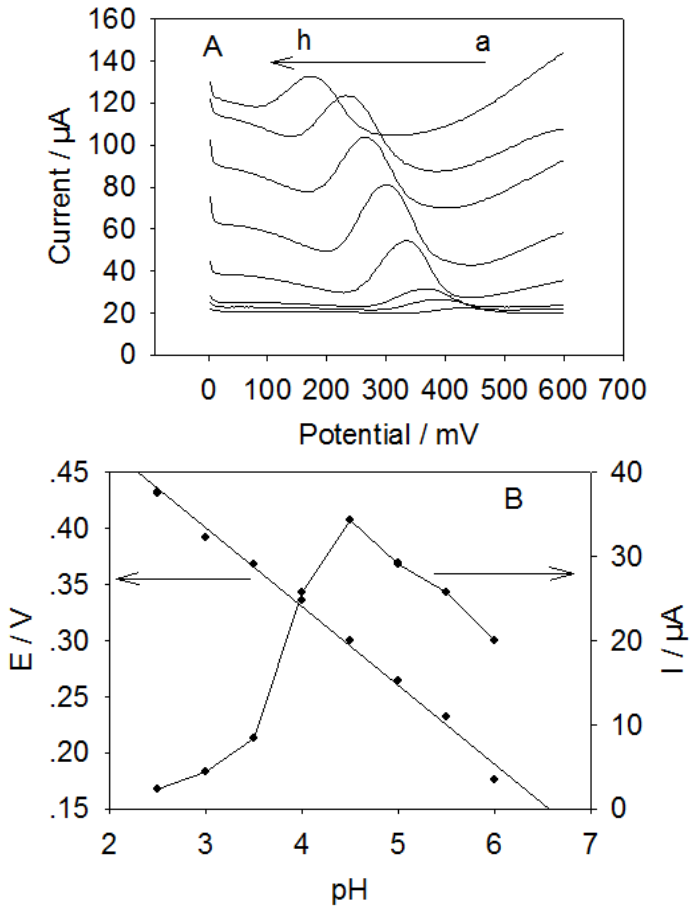

Fig. S2 (A) SWVs of 10 μM quercetin in 0.2 M ABS with different pH value (From a to h: pH 2.5, 3, 3.5, 4, 4.5, 5, 5.5, 6); (B) Effects of pH value on the peak current (Ipa) and peak potential (Epa).

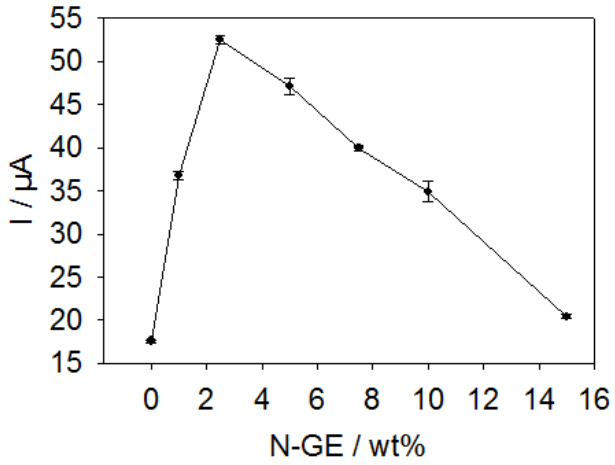

Fig. S3 Effect of the amount of N-GE in carbon paste on the oxidation peak current of 10 μM quercetin in 0.2 M ABS (pH 4.5).

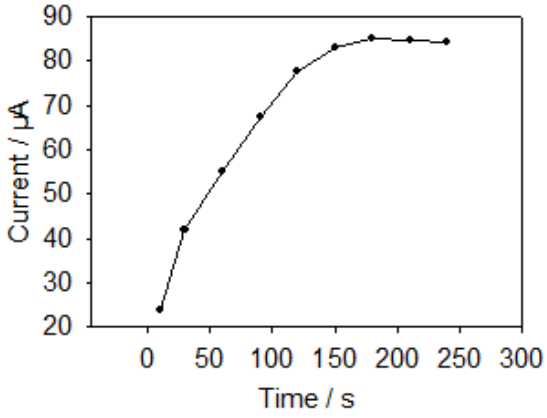

Fig. S4 Effect of accumulation time on the oxidation peak current of 10 μM quercetin in 0.2 M ABS (pH 4.5).